Carbohydrate Polymers 113 (2014) 577–587

Contents lists available at ScienceDirect

Carbohydrate Polymers

journal homepage: www.elsevier.com/locate/carbpol

2,6-Dinitroaniline and β-cyclodextrin inclusion complex properties studied by different analytical methods

Krishnan Srinivasan[a], Krishnamoorthy Sivakumar[b], Thambusamy Stalin[a,*]

[a] Department of Industrial Chemistry, School of Chemical Sciences, Alagappa University, Karaikudi 630 003, Tamilnadu, India
[b] Department of Chemistry, Sri Chandrasekharendra Saraswathi Viswa Mahavidyalaya University, Enathur, Kanchipuram 631 561, Tamilnadu, India

ARTICLE INFO

Article history:
Received 9 December 2013
Received in revised form 27 June 2014
Accepted 20 July 2014
Available online 12 August 2014

Keywords:
β-Cyclodextrin
2,6-Dinitroaniline
Inclusion complex
Patch dock server

ABSTRACT

The formation of supramolecular host-guest inclusion complex of 2,6-Dinitroaniline (2,6-DNA) with nano-hydrophobic cavity of β-cyclodextrin (β-CD) in solution phase were studied by UV-visible spectrophotometer and electrochemical method (cyclic voltammetry, CV). The prototropic behaviors of 2,6-DNA with and without β-CD and the ground state acidity constant (p*Ka*) of host-guest inclusion complex (2,6-DNA-β-CD) was studied by Spectrophotometrically. The binding constant of inclusion complex at 303 K was calculated using Benesi–Hildebrand plot and thermodynamic parameter (ΔG) were also calculated. The solid inclusion complex formation between β-CD and 2,6-DNA was confirmed by ^{1}H NMR, FT-IR, XRD and SEM analysis. The β-CD:2,6-DNA inclusion complex obtained by molecular docking studies is in good correlation with the results obtained through experimental methods.

1. Introduction

Cyclodextrins (CDs) are cyclic oligosaccharides consisting of 6, 7, and 8 units of 1,4-linked glucose units, and are named alpha (α), beta (β) and gamma (γ)-cyclodextrins, respectively (Scheme 1). These macromolecules, which can be spatially represented as a torus with wide and narrow openings corresponding to secondary and primary hydroxyl groups, respectively, can encapsulate a large variety of compounds due to the hydrophobic character of their internal cavity (Szejtli, 1998). Although the depth of the cavities for the three CDs is the same (~0.78 nm), their cavity diameters are ~0.57, 0.78 and 0.95 nm, respectively. Due to the unique chemical structure of CD molecules, the inner side of the cavity is hydrophobic and the outer side is hydrophilic. The hydrophobic nature of the CD cavities facilitates the ability of CDs to act as host for both nonpolar and polar guests, which include small molecules as well as polymers (Szejtli, 1998; Shuai, Porbeni, Wei, Shin, & Tonelli, 2001; Harada, Nishiyama, Kawaguchi, Okada, & Kamachi, 1997; Do Nascimento, Da Silva, De Torresi, Santos, & Temperini, 2002). Once the inclusion compound is formed, the stability of the guest molecules increases due to the binding forces (van der Waals attractions, hydrogen bonding, hydrophobic interactions, etc.) between the host (CDs) and guest molecules (Rekharsky & Inoue, 1998; Schneider, Hacket, & Rudiger, 1998). CDs also have several advantages in other areas, such as the food, cosmetics industries and agro chemistry (Zhang, Lerner, Rustrum, & Hofman, 1999; Loukas, Jayasekera, & Gregoriadis, 1995; Loukas, Vraka, & Gregoriadis, 1996), especially owing to their capacity to protect the guest molecules against oxidation, light-induced reaction and loss by evaporation. Additionally, they usually enhance the aqueous solubility of poorly soluble or even insoluble compounds such as organic and drug molecules (Choi, Nyongryu, Ryoo, & Pillee, 2001).

2,6-Dinitroaniline (2,6-DNA), as dinitro-substituted derivatives of aromatic amines, have become more and more significant in environmental studies due to their highly toxic nature and their suspected carcinogenic properties (Dimou, Sakkas, & Albanis, 2004; Xiang, Tong, & Lin, 2007). This 2,6-DNA was mainly used as intermediates in the synthesis of dyestuff, pharmaceuticals, pesticides, and herbicides (Kataoka, 1996), and they are released into the environment directly as industrial waste or indirectly as degradation products of herbicides and pesticides. After enter into the environment, this compound can experience complex environmental transformations at trace level, and it is very harmful to the environment potentially. Acute or chronic exposure to 2,6-DNA can produce symptoms of headache, dizziness and nausea. With the growing use of these compound in different industries, the 2,6-DNA have been included in the list of priority pollutants in many countries. In view of the environmental importance of separation of the 2,6-DNA present in the wastewaters, surface waters and other environments at trace level or ultra trace level. The β-CD can be used to separate this compound from aqueous medium by preparing their inclusion complex, because the β-CD can

* Corresponding author. Tel.: +91 9944266475; fax: +91 4565 225202.
E-mail address: drstalin76@gmail.com (T. Stalin).

http://dx.doi.org/10.1016/j.carbpol.2014.07.062
0144-8617/

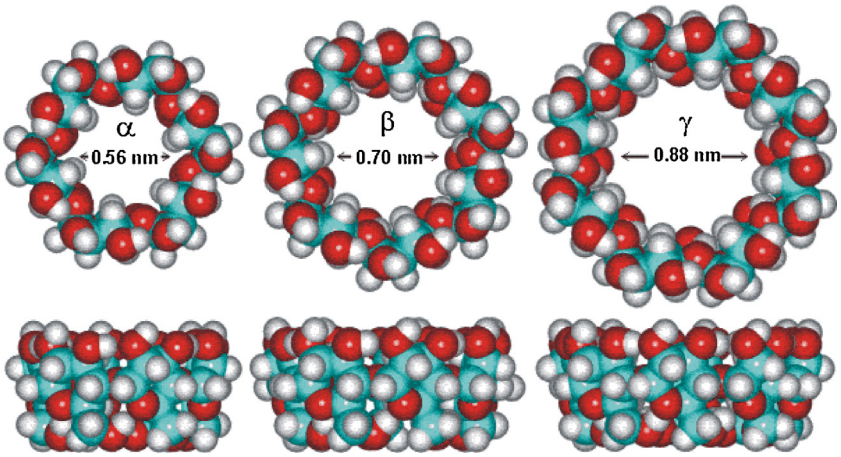

Scheme 1. 3D view of chemical structures of α-CD, β-CD and γ-CD.

selectively include the 2,6-DNA by hydrophobic interaction. 2,6-DNA is a good candidate as a model compound to characterize inclusion formation by ^{1}H NMR and FT-IR spectroscopy.

In this present study, we report the inclusion complex formation in solution phase by UV-visible spectroscopy and cyclic voltammetric technique. The solid complex were prepared and characterized by ^{1}H NMR, 2D ^{1}H NMR (ROESY), FT-IR, XRD, SEM techniques and molecular docking technique (using PatchDock server) in virtual state. We found that the virtual state analysis results correlates well with the liquid and solid-state analysis results.

2. Experimental

2.1. Instruments

The UV–vis spectra (absorption spectral measurements) were carried out with Shimadzu UV-2401PC double-beam spectrophotometer, the pH values in the range 2.0–12.0 were measured on Elico pH meter LI-120; Electrochemical studies were carried out using Auto lab electrochemical analyzer, it used to apply potential on the working electrode equipped with a three-electrode glassy carbon electrode (diameter: 1 mm) is served as a working electrode system. Reference electrode was saturated calomel electrode (SCE) and platinum wire as counter electrode. All experiments were carried out at 30 ± 1 °C. The working electrode was polished to a mirror with 0.05 μm alumina aqueous slurry, and rinsed with triply distilled water before each experiment. The supporting electrolyte was pH ~ 7 (0.1 M KH_2PO_4 + 0.1 M NaOH). 10 mg of sample were dissolved in 0.7 ml of D_2O solvent and then filtered through a Pasteur pipette, equipped with a glass wool plug that discharges into an NMR tube. Two-dimensional rotating-frame Overhauser effect spectroscopy (ROESY) experiments were performed using BRUKER-NMR 400 MHz instrument operating at 300 K and the standard Bruker program was used, DMSO-d_6 was used as a solvent, relaxation delay of 1s and mixing time 300 ms under the spin lock conditions. Powder X-ray diffraction spectra were taken by XPert PRO PANalytical diffractometer (2Theta: 0.001; minimum step size Omega: 0.001). The surface morphology was taken by Hitachi S 3000 H SEM.

2.2. Molecular docking study

The most probable structure of the 2,6-DNA:β-CD inclusion complex was determined also by molecular docking studies using the Patch Dock server (Duhovny, Inbar, Nussinov, & Wolfson, 2005). The 3D structural data of β-CD and 2,6-DNA was obtained from crystallographic databases. The guest molecule (2,6-DNA) was docked in to the host molecule (β-CD) cavity using PatchDock server by submitting the 3D coordinate data of 2,6-DNA and β-CD molecules. Docking was performed with complex type configuration settings. PatchDock server follows a geometry-based molecular docking algorithm to find the docking transformations with good molecular shape complementarily. PatchDock algorithm separates the Connolly dot surface representation (Connolly, 1983) of the molecules into concave, convex and flat patches. These divided complementary patches are matched in order to generate candidate transformations and evaluated by geometric fit and atomic desolvation energy scoring (Zhang, Vasmatzis, Cornette, & DeLisi, 1997) function. RMSD (root mean square deviation) clustering is applied to the docked solutions to select the non-redundant results and to discard redundant docking structures.

2.3. Reagents

β-Cyclodextrin {(β-CD), was obtained from Sd fine chemical company} and used without further purification. 2,6-Dinitroaniline (2,6-DNA) purchased from Alfa Aesar company. Triply distilled water was used to prepare all solutions. Solutions in the pH range 2.0–12.0 were prepared by adding the appropriate amount of NaOH and H_3PO_4. Yagil basicity scale (H_-) (Yagil, 1967) for solutions above pH ~ 12 (using a NaOH–H_2O mixture) and A modified Hammett's acidity scale (H_0) (Jorgenson & Hartter, 1963) for the solutions below pH ~ 2 (using a H_2SO_4–H_2O mixture) was employed. The solutions were prepared just before taking measurements. The concentrations of the solutions were of the order (10^{-4} to 10^{-5} mol/dm^3). The stock solution of 2,6-DNA and β-CD preparation for spectral and electrochemical studies was prepared by adopting the procedure detailed in our previous report (Stalin, Srinivasan, Vaheethabanu, & Manisankar, 2011a; Stalin, Srinivasan, Kayalvizhi, & Sivakumar, 2011b).

2.4. Preparation of solid inclusion complex of 2,6-DNA with β-CD

Accurately weighed 1 g of β-CD was placed into 50 ml conical flask and 30 ml triply distilled water added and then oscillated this solution enough. After that, 0.1774 g 2,6-DNA was put in to a 50 ml beaker and 20 ml ethanol added and put over electromagnetic stirrer to stir until it was dissolved. Then slowly poured 2,6-DNA solution into β-CD solution. The above mixed solution was continuously stirred for 48 h at room temperature and the following equilibriums can take place G (solution) + CD (solution) ↔ G-CD

Table 1
Prototropic maxima (absorption spectra) of 2,6-DNA in without and with β-CD medium and p*K*a value of 2,6-DNA (without β-CD).

Species	Without β-cyclodextrin		With β-cyclodextrin	
	λ_{max} (nm)	H_0/pH/H_-	λ_{max} (nm)	H_0/pH/H_-
Monocation	432	−4.89	–	–
	227			
	213			
Neutral	432	−4.65–15.97		0.83–15.97
	325		435	
	254		257	
	225		227	
Monoanion	–	–	–	–
p*K*a	−4.89			

(solution)⇄G-CD (solid) the first equilibrium is K_{bind}, and the second one is K_{solid}.

The reaction mixture was put and kept in to refrigerator for 48 h. At this time, we observed that yellow precipitate was formed. The precipitate was filtered by G4 crucible and washed with triply distilled water. After dried in oven at 50 °C for 12 h, yellow powder was obtained. This is solid inclusion complex of 2,6-DNA with β-CD and it further analyzed by ^{1}H NMR, 2D ^{1}H NMR (ROESY), FT-IR, XRD and SEM analysis.

3. Results and discussion

3.1. Effect of pH

The absorption spectra of 2,6-DNA were recorded at different pH solution and the relevant data are compiled in Table 1 and Fig. 1. In the pH range 2.0–12. Absorption maxima nearly resemble the spectra observed in non-aqueous solvents and thus can be assigned to the neutral species. In the pH range −4.65 (H_0) to pH ∼ 12 the absorption maxima were observed at 432 nm. With a decrease on pH from 7.0, there is no change in the absorption maxima up to in −4.65 solution. The absorption intensity is decreases at 432 nm in H_0 −4.85 this is due to the formation of monocation. The absorption intensity is decreases due to the protanation with lone pair of electrons present on the amine group and also removal of conjugation by the presence of electron withdrawing group (—NO_2) in two adjacent side (*ortho* position). In the case of 2,6-DNA (neutral), absorption maxima observed at 432 nm because of lone pair of electrons on N atom is in conjugation with the π-bond system of the benzene ring. In alkali medium, there is no change in absorption maxima even in −4.65. So there is no formation of monoanion; due to deprotanation is not possible, because the nitro groups are present in the *ortho* position and it makes steric hindrance to amine group, so that the formation of monoanion was restricted. The prototropic equilibrium is shown in Scheme 2. The p*K*a value for the equilibria is determined spectrophotometrically and is given in Table 1.

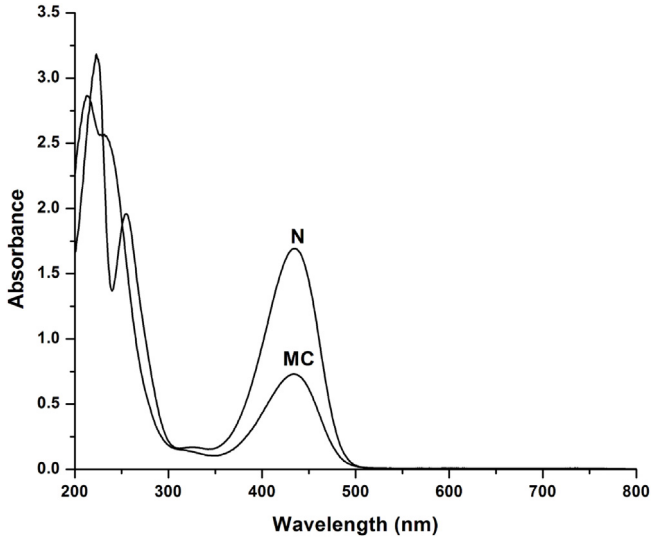

Fig. 1. Absorption spectra of different prototropic species of 2,6-DNA at 303 K; concentration 2×10^{-4} M (MC) monocation and (N) neutral.

Table 2
Absorption maxima (nm) and log ε of 2,6-DNA at different concentrations of β-CD in pH ∼ 7 solution.

S. No.	Concentration of β-CD (M)	pH ∼ 7	
		λ_{max} (nm)	Log ε
1	0	432	3.94
		254	4.01
		225	4.20
2	0.002	433	3.95
		225	4.03
		225	4.23
3	0.004	433	3.95
		255	4.06
		226	4.24
4	0.006	433	3.95
		256	4.07
		226	4.24
5	0.008	434	3.95
		256	4.08
		226	4.25
6	0.010	434	3.96
		256	4.09
		228	4.25
7	0.012	435	3.96
		257	4.11
		227	4.26
Binding constant (M^{-1})		17.8	
Δ*G* (kJ/mol)		−7.25	

3.2. Effect of β-cyclodextrin

Table 2 and Fig. 2 show the absorption maxima of 2,6-DNA (2×10^{-4} mol/dm^3) in pH ∼ 7 (neutral) solution containing different concentrations of β-CD. At pH ∼ 7, 2,6-DNA exists as a neutral form only. In pH ∼ 7, no clear isosbestic point was observed in the

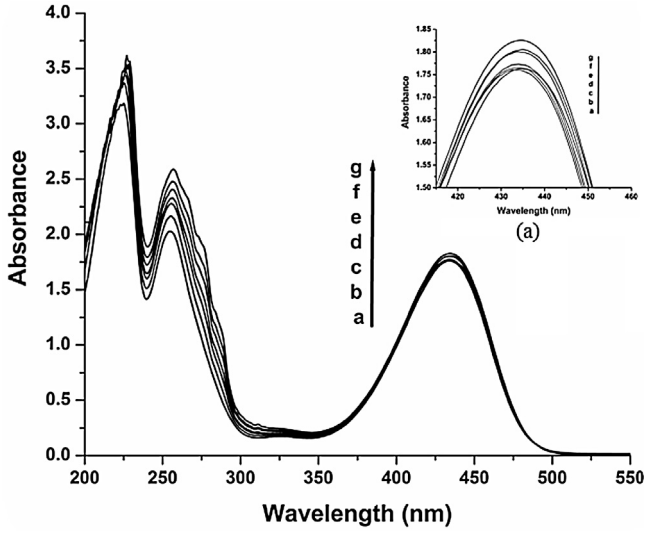

Fig. 2. Absorption spectra of 2,6-DNA (conc. 2×10^{-4} M) in pH ∼ 7 solutions at different β-CD ((a)–(g) conc. 0–12×10^{-3} M). Inset (a) magnified view of β-CD effect in pH ∼ 7 solution at 432 nm.

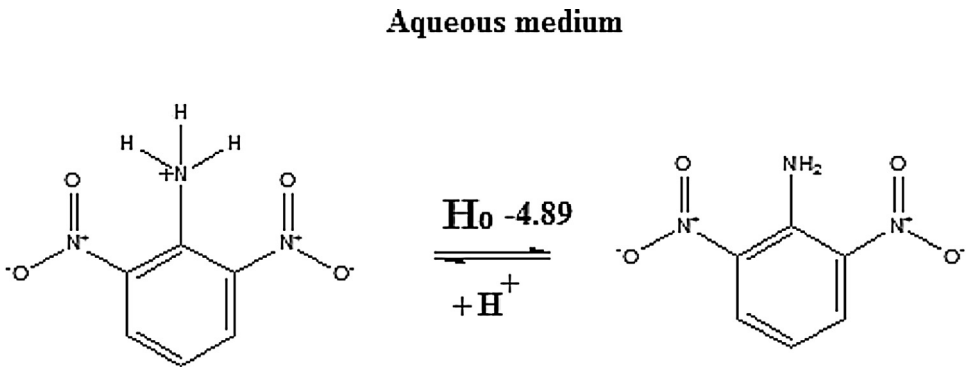

Scheme 2. Prototropic equilibria of 2,6-DNA in aqueous medium.

absorption spectra even in the presence of higher β-CD concentration.

In pH ~ 7 solution the absorption maxima is increased and 1:1 inclusion complex is formed, whereas the absorption spectra of 2,6-DNA in pH ~ 7 there was slight red shift in the absorption maxima was observed and also the absorption intensity was increased when increasing the β-CD concentration. At pH ~ 7, 2,6-DNA exist as neutral form only with 1:1 complex form, In pH ~ 7 the 2,6-DNA located inside the β-CD cavity and the NH_2 group located at above the β-CD rim, which will cause the increase of the absorbance. This behavior has been attributed to the enhanced dissolution of the 2,6-DNA molecule through the hydrophobic interaction between 2,6-DNA and β-CD. These results indicate that 2,6-DNA molecule is entrapped into β-CD cavity to form an inclusion complex. The binding constant for the formation of 2,6-DNA:β-CD complex has been determined by analyzing the changes in the intensity of absorbance with the β-CD concentration. Fig. S1 plotting $1/(A - A_0)$ versus 1/[β-CD] for a 1:1 host:guest inclusion complex. In 1:1 inclusion complex gives straight line at pH ~ 7. The binding constant (K) can be obtained by using the modified Benesi–Hildebrand equation (Benesi & Hildebrand, 1949) for the 1:1 complex Eq. (1) between 2,6-DNA and β-CD as shown below.

$$\frac{1}{(A - A_0)} = \frac{1}{\Delta\varepsilon} + \frac{1}{K[2,6-\mathrm{DNA}]_0\,\Delta\varepsilon\left[\beta - CD\right]_0} \quad (1)$$

where $A - A_0$ is the difference between the absorbance of 2,6-DNA in the presence and absence of β-CD, $\Delta\varepsilon$ is the difference between the molar absorption coefficient of 2,6-DNA and the inclusion complex $[2,6\text{-DNA}]_0$ and $[\beta\text{-CD}]_0$ are the initial concentration of 2,6-DNA and β-CD, respectively. A good correlation was obtained for pH ~ 7 (Fig. S1, $R^2 = 0.9576$), it's also confirm that the formation of 1:1 inclusion complex. From the intercept and slope value of this plot K was calculated [pH ~ 7 = 17.8 M^{-1}] at 303 K (Table 2). The determination of the thermodynamic parameter for inclusion process change in the free energy (ΔG) can be calculated from the binding constant 'K' by the following the following equation:

$$\Delta G = -RT \ln K \quad (2)$$

The thermodynamic parameter ΔG, for the binding of the guest molecule to β-CD cavity is given in Table 2. As can be seen from Table 2, ΔG is negative which suggests that the inclusion process proceeded spontaneously at 303 K. This indicates that the formation of inclusion complex is an exergonic process.

3.3. Possible inclusion complex of 2,6-DNA in β-CD cavity

In 1:1 inclusion complex, the aromatic moiety is embedded in β-CD cavity and the NH_2 group present above the β-CD rim. The formation of the 1:1 host:guest complex is clearly demonstrated

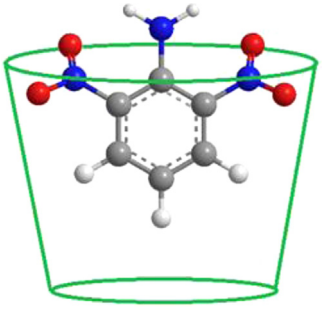

Scheme 3. The proposed structure of inclusion complex of (a) 2,6-DNA with β-CD. The oxygen atoms are shown as red, nitrogen as blue and carbon as gray color, hydrogen atoms are white.

in Scheme 3. Such 1:1 inclusion complex structure gains further stabilization energy by releasing of water from hydrophobic cavity. The inclusion complex has further stabilized by the interaction of lone pair electrons of secondary hydroxyl group of β-CD with π electrons (benzenoid) of 2,6-DNA. The pH dependent changes in the absorption of the 2,6-DNA molecule in β-CD solution have also been recorded (Table 1). Even in higher alkali (H_15.65) medium there is no formation of monoanion in β-CD medium which was same behavior as without β-CD medium, due to the 2,6-DNA was included into the nano hydrophobic cavity of β-CD and the NH_2 group present above the β-CD rim. To substantiate the above discussion, the effect of β-CD on the prototropic equilibrium, the 2,6-DNA is present as neutral in pH range −4.65 (H_0) to H_15.65. The absorption spectra of 2,6-DNA in ground state shows the pH range {−4.65 (H_0) to 15.65(H_)} as neutral form, neutral to monocation (without β-CD) are hyperchromic effect is observed and neutral pH red slight shifted in β-CD medium this was similar to its in aqueous medium (Scheme 2), its indicating 2,6-DNA molecule entrapped in β-CD cavity.

3.4. Semi empirical quantum mechanical calculations

The internal diameter of the β-CD is approximately 6.5 Å and its height is 7.8 Å (Scheme 4). Considering the shape and dimensions of β-CD, the ground state of 2,6-DNA molecules were optimized using AM1 method (Scheme 4). In 2,6-DNA; the vertical distances between H_{14}–H_{17} and H_{15}–H_{17} is 5.8 Å. The horizontal distance between O_9–O_{12} is 7.1 Å, O_{10}–O_{12} and O_9–O_{13} is 6.3 Å. The vertical distance and the horizontal distance measured from the terminal atoms of 2,6-DNA are less than the height and vertical diameter of β-CD. Since, the height of 2,6-DNA are lower than upper-lower rim

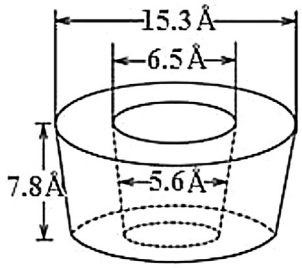

(a)

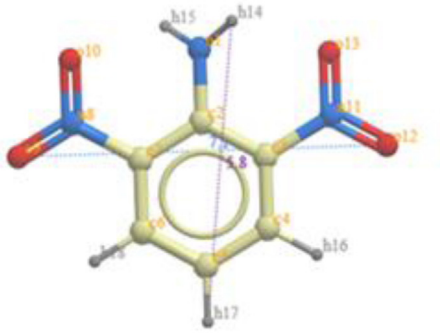

(b)

2,6-DNA bond distance in Å		Orientation
H_{14} - H_{17}	5.8	Vertical
H_{15} - H_{17}	5.8	Vertical
O_9 - O_{12}	7.1	Horizonal
O_{10} - O_{12}	6.3	Horizonal
O_9 - O_{13}	6.3	Horizonal

Scheme 4. Schematic representation of semi empirical bond distance of (a) β-CD, (b) 2,6-DNA. (For interpretation of the references to color in this scheme legend, the reader is referred to the web version of this article.)

of β-CD, the insertion of 2,6-DNA in the β-CD cavity is possible as shown in Scheme 3.

3.5. Molecular docking studies of inclusion process

The 3D structure of 2,6-DNA was obtained from crystallographic databases are shown in Scheme 5(a). The guest molecules of 2,6-DNA was docked into the cavity of β-CD using PatchDock server. The PatchDock server program gave several possible docked models for the most probable structure based on the energetic parameters; geometric shape complementarity score, approximate interface area size and atomic contact energy of the 2,6-DNA:β-CD inclusion complexes. The docked 2,6-DNA:β-CD 1:1 model (Scheme 5b) with the highest geometric shape complementarity score 2346 for 2,6-DNA:β-CD, the approximate interface area size of 243.3 $Å^2$ for 2,6-DNA:β-CD and atomic contact energy of −850 kJ/mol for 2,6-DNA:β-CD was calculated. This is highly probable and energetically favorable model and it was in good correlation with results obtained through experimental methods.

Table 3
CV for 2,6-DNA:β-CD in pH ~ 7 buffer solution, scan rate 100 mV/s, 2,6-DNA (conc. 2×10^{-4} M) and (a–g) $0–12\times10^{-3}$ M β-CD concentrations.

Concentration of β-CD (M)	pH ~ 7			
	E_{pa} (V)	I_{pa} (μA)	E_{pc} (V)	I_{pc} (μA)
0	0.197	7.262	−0.630	−16.92
			−0.816	−16.04
0.002	0.200	6.888	−0.630	−17.50
			−0.818	−16.59
0.004	0.205	6.637	−0.633	−18.78
			−0.823	−17.16
0.006	0.234	6.201	−0.633	−19.13
			−0.826	−18.21
0.008	0.234	5.675	−0.635	−19.33
			−0.826	−18.42
0.010	0.234	5.438	−0.635	−20.86
			−0.826	−19.35
0.012	0.258	4.934	−0.638	−21.09
			−0.828	−19.99
Binding constant (M^{-1})	66			
ΔG (kJ/mol)	−10.5			

3.6. Electrochemical studies

The cyclic voltammograms (CV) show the electrochemical behavior of 2,6-DNA in pH ~ 7 with β-CD (Table 3 and Fig. 3). Formation of the inclusion complex of 2,6-DNA with β-CD were also confirmed by electrochemical method. In pH ~ 7 the cyclic voltammograms shows an anodic peak during the forward scan (toward positive potential) at 0.197 V and two reduction peaks during the reverse scan (toward negative potential) at −0.630 V and −0.816 V. These peaks are ascribed as oxidation of 2,6-DNA (NH_2; 0.197 V) and the reduction of anilinum anion (−0.630 V) into NH_2 with another one reduction peak of NO_2 (−816 V) into hydroxylamine.

The redox behaviors of both 2,6-DNA were clearly represented in Scheme 6. The cathodic peak current (i_{pc}) of 2,6-DNA (Table 3 and Fig. 3) was increased with increasing the β-CD concentration in pH ~ 7. The cathodic peak potential (E_{pc}), shifted toward positive direction in pH ~ 7. This result shows that the inclusion complex between 2,6-DNA and β-CD was formed when 2,6-DNA was added into β-CD aqueous solution. In addition, the cathodic peak current increases with increasing β-CD concentration; this is due to the nitro groups are present inside of the β-CD cavity and the catalytic behavior of β-CD to the included guest molecule.

The binding constant (K) and stoichiometric ratio of the inclusion complex of 2,6-DNA can be determined according to the

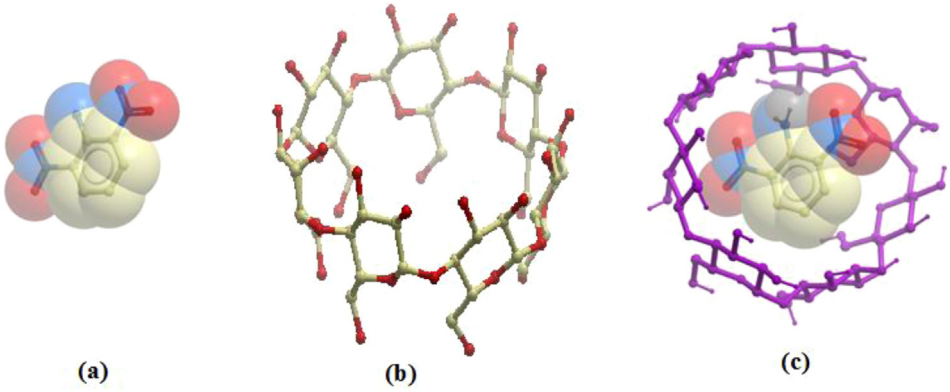

Scheme 5. Ball and stick representation of (a) 2,6-DNA (b) β-CD (c)2,6-DNA:β-CD inclusion complex; the oxygen atoms are shown as red ball, nitrogen as blue and carbon as gray balls; hydrogen atoms are white balls. (For interpretation of the references to color in this scheme legend, the reader is referred to the web version of this article.)

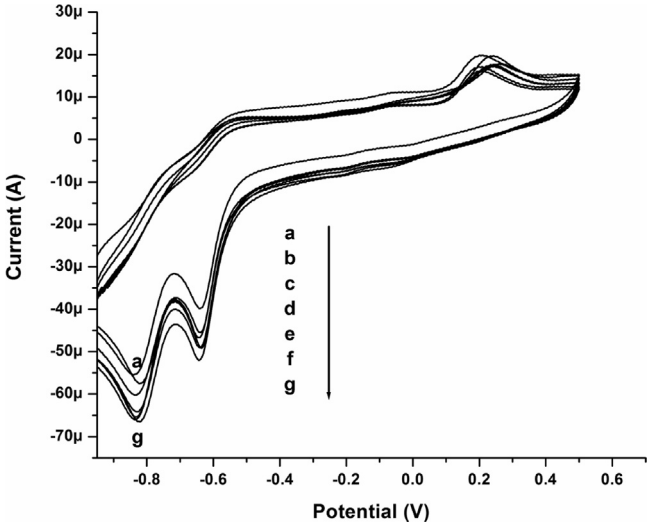

Fig. 3. Cyclic voltammograms for 2,6-DNA:β-CD in pH ~ 7 buffer solution, scan rate 100 mV/s, 2,6-DNA (conc. 2×10^{-4} M) and β-CD ((a)–(g) conc. 0–12×10^{-3} M).

Benesi–Hildebrand (14) relation assuming the formation of a 1:1 host–guest complex.

$$\frac{1}{I_{HG} - I_G} = \frac{1}{\Delta I} + \frac{1}{K[2,6\text{-DNA}]_0 \, \Delta I \left[\beta\text{-CD}\right]_0} \quad (3)$$

where I_G is the reduction peak current of guest molecule of 2,6-DNA, and I_{HG} is the reduction peak current of inclusion complex of 2,6-DNA:β-CD. $I_{HG} - I_G$ is the difference between the reduction peak current of inclusion complex and 2,6-DNA. ΔI is the difference between the molar peak current coefficient of the inclusion complex and 2,6-DNA. The $[2,6\text{-DNA}]_0$ and $[\beta\text{-CD}]_0$ are the initial concentration of 2,6-DNA and β-CD, respectively. Plot of $[1/I_{HG} - I_G]$ verses 1/[β-CD] gives a straight line in pH ~ 7 solution as shown in Fig. S2. Good linear correlation was obtained (R^2 = 0. 9945, pH ~ 7), it's also confirm that the formation of a 1:1 inclusion complex for pH ~ 7 solution. From the intercept and slope values of this plot K was evaluated, the binding constant values for 2,6-DNA:β-CD is 66 M^{-1} in pH ~ 7. This value indicate that 2,6-DNA molecule is encapsulated in the β-CD cavity to form an inclusion complex.

3.7. ^1H NMR studies of 2,6-DNA with β-CD

The formation of solid inclusion complex can be analyzed from ^{1}H NMR spectra (Chen, Diao, & Zhang, 2006). Fig. 4 showed the typical ^{1}H NMR spectra of (a) β-CD, (b) the solid inclusion complex of 2,6-DNA with β-CD (chemical shift changes with β-CD), (c) 2,6-DNA and (d) the solid inclusion complex (chemical shift changes with 2,6-DNA). 10 mg of sample were dissolved in 0.7 ml of D_2O solvent and then filtered through a Pasteur pipette, equipped with a glass wool plug that discharges into an NMR tube. The values of chemical shifts, δ for different protons in β-CD with solid inclusion complex and 2,6-DNA with solid inclusion complex were listed in Tables 4 and 5. It can be seen from the ^{1}H NMR that in solid inclusion complex, a great upfield shift was occurred for H_3 and H_5 protons of β-CD experience magnetic perturbation due to the guest molecule while those at the H_2 and H_4 positions have no significant change in the chemical shift. Which (H_3 and H_5) locate in the nano hydrophobic cavity of β-CD (Scheme 7b). The changes of chemical shift ($\Delta\delta$) of H_3 and H_5 suggested that the 2,6-DNA monomer entered into the nano hydrophobic cavity of β-CD. The phenyl ring of 2,6-DNA made the signals of β-CD protons (H_3 and H_5) upfield shift. On the contrary, the chemical shifts of H_1, H_2, H_4, and H_{6ab}, which are on the outer surface of β-CD and the narrow opening of β-CD as shown as in Scheme 7b, were only slightly affected by the guest molecule. Similarly, the chemical shifts of H_a, H_b and H_c of 2,6-DNA (Scheme 7c) locate in the nano hydrophobic cavity of β-CD was also moved in upfield significantly because the interaction between hydrophobic interactions of aromatic ring of the 2,6-DNA and hydrogen atoms in the β-CD cavity should be present in the complex. Since the C—H bonds of positions 3 and 5 of the

Table 4
^{1}H NMR chemical shifts of β-CD in free and complexed state determined in D_2O at 303 K.

Protons	β-CD	2,6-DNA:β-CD	$\Delta\delta$
	δ (ppm)	δ (ppm)	
H_1	4.966	4.964	−0.002
H_2	3.554	3.553	−0.002
H_3	3.877	3.860	−0.017
H_4	3.535	3.476	−0.002
H_5	3.748	3.736	−0.012
H_6	3.797	3.796	−0.001

Table 5
^{1}H NMR chemical shifts of 2,6-DNA in free and complexed state determined in D_2O at 300 K.

Substances	H_a δ (ppm)	H_b δ (ppm)	H_c δ (ppm)
2,6-DNA	8.335	–	7.080
2,6-DNA:β-CD	8.285	–	6.996
$\Delta\delta$	−0.050	–	−0.084

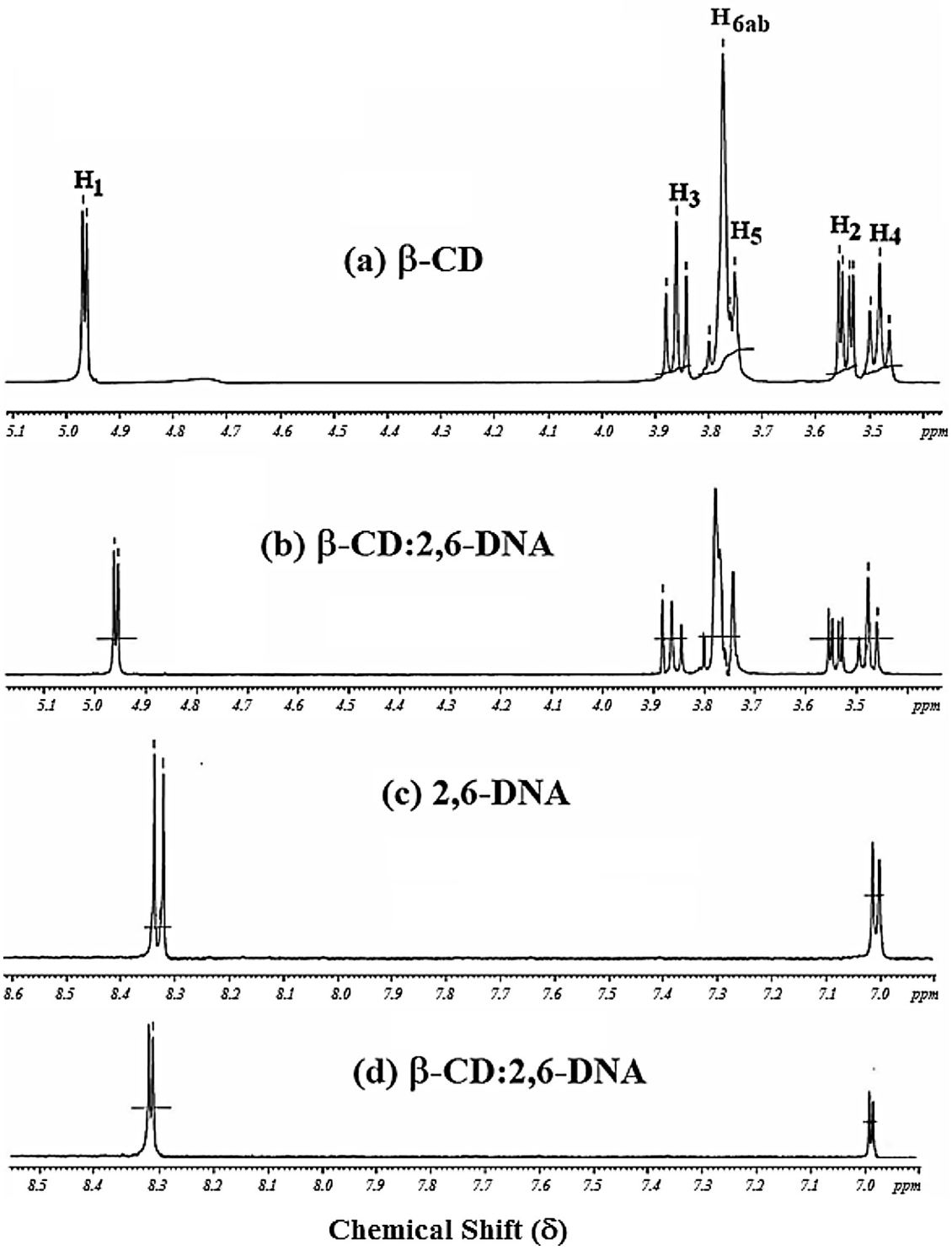

Fig. 4. ^{1}H NMR spectra of (a) β-CD, (b) the solid complex (chemical shift with respect to β-CD); (c) 2,6-DNA, (d) the solid complex (chemical shift with respect to 2,6-DNA).

glucopyranosyl unit point toward the β-CD cavity, shielding effects due to the aromatic ring current should influence the chemical shifts of the host protons. The upfield-shifted signals of H_3 and H_5 suggested that the majority of those protons should not be exactly in the plane of the ring current. The H_2 and H_4 protons do not directly interact with 2,6-DNA because they are exposed to bulk environments. The significant distinguish for these ^{1}H NMR spectra strongly confirmed that the solid inclusion complex formation of 2,6-DNA with β-CD.

3.8. 2D ^{1}H NMR (ROESY) studies of 2,6-DNA with β-CD

The 2D ^{1}H NMR (ROESY) is a powerful technique for investigation of inter and intra molecular interactions. The chemical shift changes was shown by H_a, and H_c protons of aromatic (hydrophobic part) moiety (Sohajda et al., 2009) of 2,6-DNA may play a major role in the inclusion process. To verify this hypothesis, 2D ^{1}H NMR spectra were recorded. The presence of NOE cross-peaks between protons of two different species in 2D ^{1}H NMR spectra is an indication

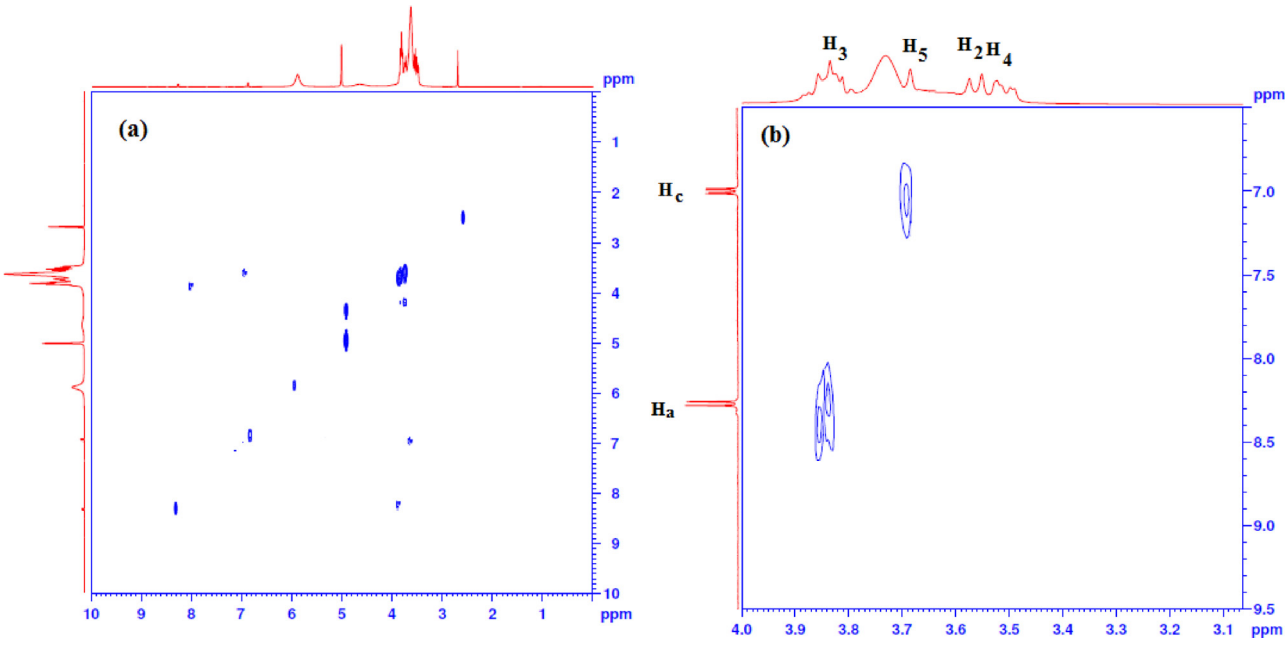

Fig. 5. The 2D ^{1}H NMR (ROESY) spectra of inclusion complex of (a) 2,6-DNA:β-CD, (b) partial counter plot of 2,6-DNA:β-CD in DMSO-d_6 at 300 K.

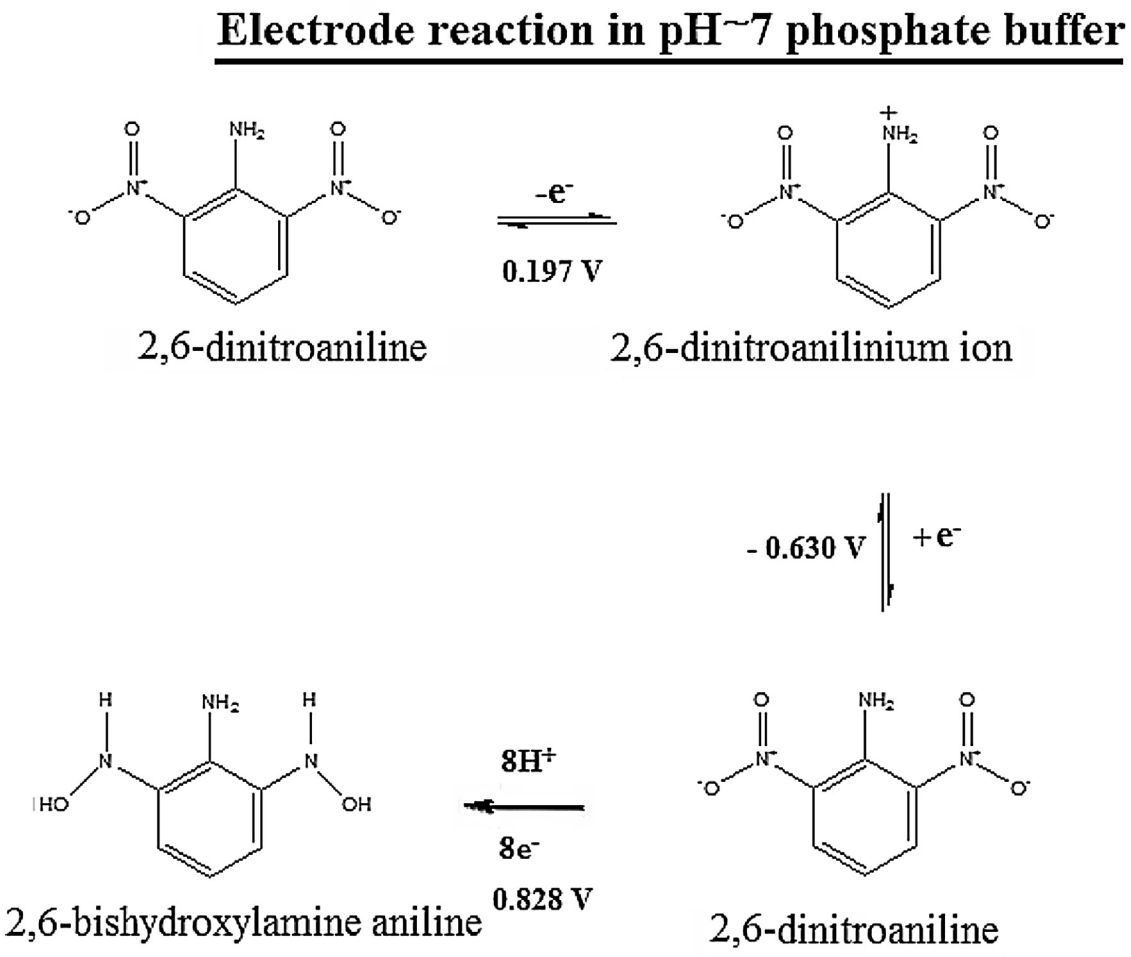

Scheme 6. Reaction mechanism of 2,6-DNA in pH ~ 7 buffer solution at glassy carbon electrode.

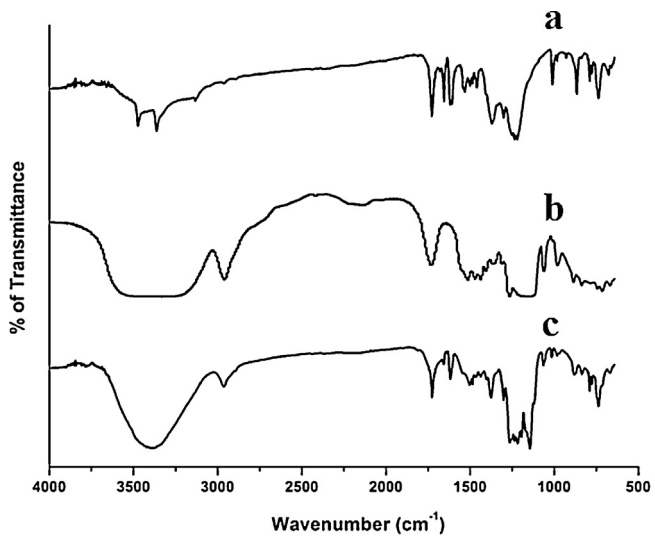

Fig. 6. FT-IR Spectra of (a) 2,6-DNA, (b) β-CD and (c) solid inclusion complex of 2,6-DNA:β-CD complex in KBr.

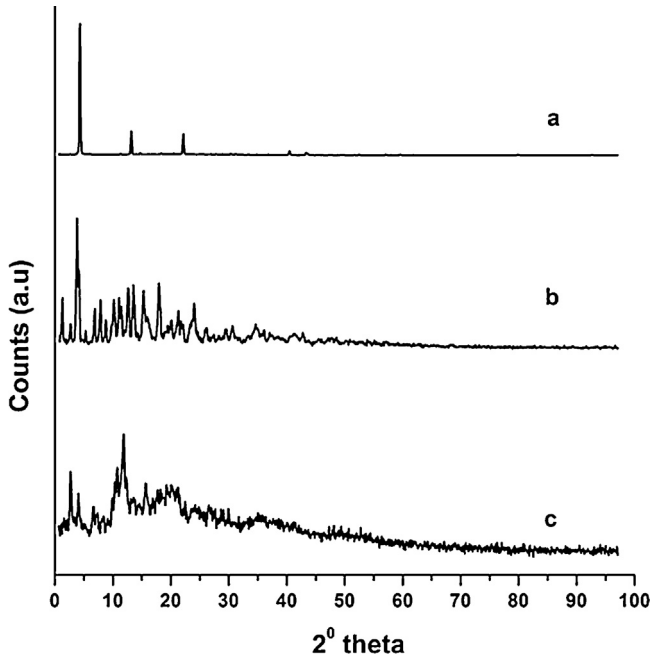

Fig. 7. Powder X Ray diffraction spectra of (a) 2,6-DNA, (b) β-CD and (c) solid inclusion complex of 2,6-DNA:β-CD.

that they are in spatial contact through space within the cavity of β-CD. Fig. 5 shows the 2D spectra of (a) 2,6-DNA:β-CD and (b) counter part of 2,6-DNA:β-CD systems, two groups of intermolecular NOE cross-peaks were observed.

In 2,6-DNA:β-CD complex two groups of inter molecular NOE cross peaks were observed. The first NOE cross peak belongs to the interaction between the H_3 (3.860 ppm) proton of β-CD with the meta positioned protons (8.285 ppm) of 2,6-DNA and the another NOE cross peak was assigned the interaction between the H_5 protons (3.736 ppm) of β-CD with the *para* positioned proton (6.996 ppm) of 2,6-DNA indicates their proximity. In all cases the interaction of 2,6-DNA with only internal protons of β-CD (H_3 & H_5) were observed. In addition the H_{6ab} protons of β-CD were not affected by the inclusion process. So that we can confirmed that the 2,6-DNA is included in to the β-CD cavity via wider rim. From the above fact the 2,6-DNA are interact with β-CD through space contact, not by bonding.

3.9. FT-IR spectral studies

The solid inclusion complex formation has been confirmed by FT-IR spectroscopy, because the bands resulting from the included part of the guest molecule are generally shifted or their intensities altered. Fig. 6 is the FT-IR spectra of (a) β-CD, (b) 2,6-DNA, (c) solid inclusion complex of 2,6-DNA.

From the Fig. 6 the two characteristic stretching of -NO_2 peaks were observed at 1562 cm^{-1}, 1359 cm^{-1}. These stretching bands were shifted to 1564 cm^{-1}, 1365 cm^{-1} and also the intensity of these peaks were reduced this is due to the nitro group of 2,6-DNA was present (included) in the nanocavity of β-CD. The characteristics stretching of C—N (—NH) appeared at 1265 cm^{-1} and its shifted to 1269 cm^{-1}, this is due to the phenyl ring of 2,6-DNA was present into the nanocavity of β-CD. The stretching band of C—N (—NO_2) group appeared at 889 cm^{-1} and it shifted to 892 cm^{-1} and also its intensity was reduced, because of the nitro group was entrapped into the nanocavity of β-CD. The stretching vibration of —C=C— appeared at 1635 cm^{-1} and it shifted to 1637 cm^{-1}, and its intensity also reduced, due to the hydrophobic part of benzene ring of 2,6-DNA was included into the nanocavity of β-CD. As can be seen above discussions it can be concluded that of 2,6-DNA molecule was included into β-CD cavity.

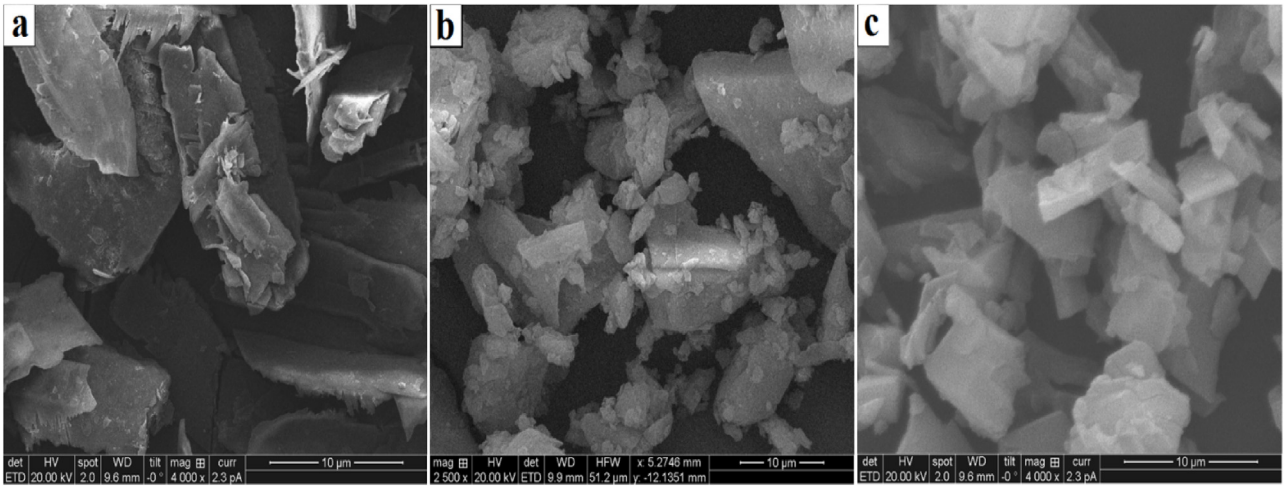

Fig. 8. Scanning electron microscope photographs (Pt. coated) of (a) 2,6-DNA (b) β-CD and (c) solid inclusion complex of 2,6-DNA:β-CD.

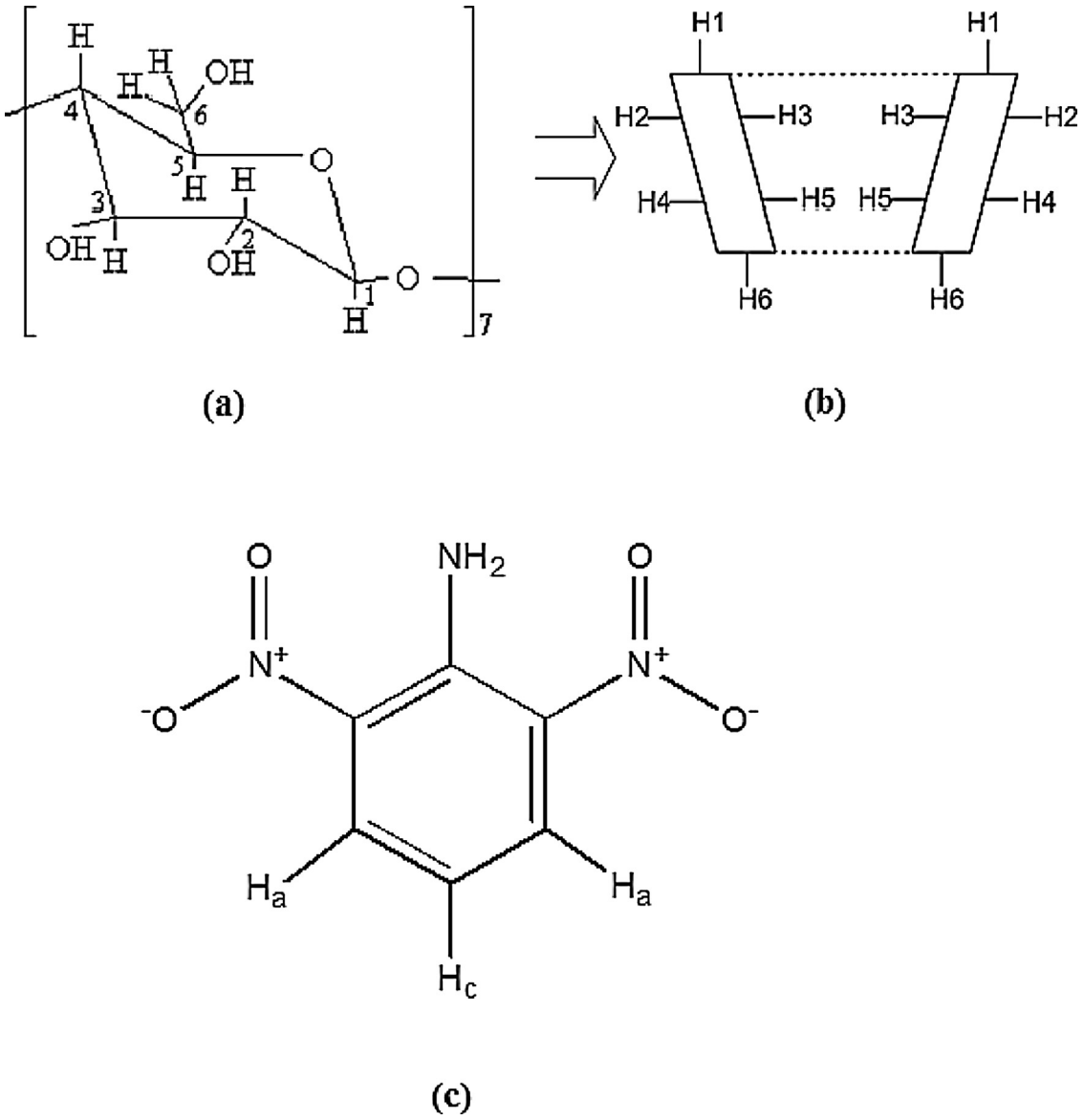

Scheme 7. (a) The stereo-configuration of β-CD, (b) truncated-cone shape of β-CD and (c) 2,6-DNA.

3.10. Powder X-ray diffraction pattern

The lack of crystallinity is an added evidence for the formation of inclusion complex (Williams, Mahaguna, & Sriwongjanya, 1998). Fig. 7 shows the XRD patterns for guest (2,6-DNA), host (β-CD) and their complex systems were prepared by co-precipitation techniques at molar ratio of 1:1. The powder X-ray diffraction pattern of 2,6-DNA (Fig. 7a) revealed that several sharp high intensity peaks at different diffraction angles (2θ) of 12.64, 19.07, 25.57, and 38.84 suggesting that the 2,6-DNA existed as crystalline nature. The β-CD (Fig. 7b) showed a crystalline diffractogram, while a diffuse halo-pattern was recorded for 2,6-DNA-β-CD (Fig. 7c) demonstrating its amorphous nature. The diffraction patterns of the investigated in the complex correspond to the correct position of those of the pure components. The lower intensities of the diffraction peaks indicate that the particle sizes were reduced during complex preparation in solution phase of the pure crystalline components. Few of diffraction peaks of 2,6-DNA was matches with those of β-CD was evident. A typical diffuse pattern indicating the entirely amorphous nature of 2,6-DNA in complexed state.

3.11. Scanning electron microscope morphological observations

Scanning electron microscope (SEM) are well suited for visualize the surface texture of the deposited film. The SEM analysis is ideal for quantitatively measuring the surface roughness and for visualizing the surface texture of the substance. First we observed surface morphological structure of (a) 2,6-DNA,(b) β-CD (Fig. 8) by SEM, and then we also observed the surface morphological structure of (c) solid inclusion complex (Fig. 8c). These pictures clearly elucidated the difference of each other. Modification of crystals can be assumed as a proof of the formation of a solid inclusion complex with nano hydrophobic cavity of β-CD.

4. Conclusions

The following conclusion can be arrived at from the above studies: (i) The ground state acidity constant (p*K*a) value for prototropic reaction of 2,6-DNA was calculated in absence of β-CD by spectrophotometricaly. (ii) 2,6-DNA forms 1:1 inclusion complex with β-CD in pH ~ 7. (iv) The electrochemical studies also confirmed the

formation of inclusion complex in pH ~ 7 (v) ^{1}H NMR, 2D ^{1}H NMR (ROESY), FT-IR, XRD and SEM results suggest 2,6-DNA formed a solid inclusion complex with nano hydrophobic cavity of β-CD. (vi) The energetically favorable complex obtained by molecular docking studies is in good correlation with the inclusion model predicted through experimental investigations.

Acknowledgements

One of the authors K. Srinivasan acknowledges to UGC-BSR for providing Research Fellowship (AU/UGC-BSR/IC/1069/2011) for Science Meritorious student.

Appendix A. Supplementary data

Supplementary data associated with this article can be found, in the online version, at http://dx.doi.org/10.1016/j.carbpol.2014.07.062.

References

Szejtli, J. (1998). *Chemical Reviews*, *98*, 1743–1753.
Shuai, X. T., Porbeni, F. E., Wei, M., Shin, I. D., & Tonelli, A. E. (2001). *Macromolecules*, *34*, 7355–7361.
Harada, A., Nishiyama, T., Kawaguchi, Y., Okada, M., & Kamachi, M. (1997). *Macromolecules*, *30*, 7115–7118.
Do Nascimento, G. M., Da Silva, J. E. P., De Torresi, S. I. C., Santos, P. S., & Temperini, M. L. A. (2002). *Molecular Crystals & Liquid Crystals*, *53*, 374–379.
Rekharsky, M. V., & Inoue, Y. (1998). *Chemical Reviews*, *98*, 1875–1917.
Schneider, H. J., Hacket, F., & Rudiger, V. (1998). *Chemical Reviews*, *98*, 1755–1786.
Zhang, L., Lerner, S., Rustrum, W. V., & Hofman, G. A. (1999). *Bioelectrochemistry and Bioenergetics*, *48*, 453–461.
Loukas, Y. L., Jayasekera, P., & Gregoriadis, G. (1995). *International Journal of Pharmaceutics*, *117*, 85–94.
Loukas, Y. L., Vraka, V., & Gregoriadis, G. (1996). *International Journal of Pharmaceutics*, *144*, 225–231.
Choi, S. H., Nyongryu, E., Ryoo, J., & Pillee, K. (2001). *Journal of Inclusion Phenomena*, *40*, 271–274.
Dimou, A. D., Sakkas, V. A., & Albanis, T. A. (2004). *International Journal of Environmental Analytical Chemistry*, *84*, 173–182.
Xiang, G. H., Tong, C. L., & Lin, H. Z. (2007). *Journal of Fluorescence*, *17*, 512–521.
Kataoka, H. (1996). *Journal of Chromatography A*, *733*, 19–34.
Duhovny, D. S., Inbar, Y., Nussinov, R., & Wolfson, H. J. (2005). *Nucleic Acids Research*, *33*, 363–367.
Connolly, M. L. (1983). *Journal of Applied Crystallography*, *16*, 548–558.
Zhang, C., Vasmatzis, G., Cornette, J. L., & DeLisi, C. (1997). *Journal of Molecular Biology*, *267*, 707–726.
Yagil, G. (1967). *Journal of Physical Chemistry*, *71*, 1034–1044.
Jorgenson, M. J., & Hartter, D. R. (1963). *Journal of the American Chemical Society*, *85*, 878–883.
Stalin, T., Srinivasan, K., Vaheethabanu, J., & Manisankar, P. (2011). *Journal of Molecular Structure*, *987*, 214–224.
Stalin, T., Srinivasan, K., Kayalvizhi, K., & Sivakumar, K. (2011). *Spectrochimica Acta, A: Molecular and Biomolecular Spectroscopy*, *79*, 169–178.
Benesi, H. A., & Hildebrand, J. H. (1949). *Journal of the American Chemical Society*, *71*, 2703–2707.
Chen, M., Diao, G., & Zhang, E. (2006). *Chemosphere*, *63*, 522–529.
Sohajda, T., Beni, S., Varga, E., Ivanyi, R., Racz, A., Szente, L., & Noszal, B. (2009). *Journal of Pharmaceutical and Biomedical Analysis*, *50*, 737–745.
Williams, R. O., Mahaguna, V., & Sriwongjanya, M. (1998). *European Journal of Pharmaceutics and Biopharmaceutics*, *46*, 355–360.